第 34 卷第 12 期
2018 年 12 月

无 机 化 学 学 报
CHINESE JOURNAL OF INORGANIC CHEMISTRY

Vol.34 No.12
2254-2260

通过棒状金属羧酸/羟基次级结构单元形成的锌金属有机骨架的低温余晖性质

汪鹏飞*,[1,2] 汪丽君[1]

([1]池州学院化学与材料工程学院,池州 247000)

([2]南京大学配位化学国家重点实验室,南京 210023)

摘要：通过一个含 3 个羧基基团的多功能配体 2-羟基-1,3,5-苯基三羧酸(HO-H_3BTC)与锌盐构筑了一个三维多孔锌骨架结构配合物,{[Zn_4(O-BTC)$_2$(H_2O)$_5$]·2DMF·0.5H_2O}$_n$ (**1**)。通过单晶 X 射线衍射、粉末 X 射线衍射、元素分析、红外光谱、热重分析以及固体紫外吸收光谱对该配合物进行了表征。配合物 **1** 是通过棒状金属锌–羧酸/羟基次级结构单元构筑的一个三维骨架结构,其在室温下显示强烈的蓝色荧光。此外,在低温条件下(10 K)配合物 **1** 显示余晖性质。

关键词：金属有机框架；棒状金属次级结构单元；荧光性质；余晖

中图分类号：O614.24+1 **文献标识码**：A **文章编号**：1001-4861(2018)12-2254-07

DOI:10.11862/CJIC.2018.246

Zn-Based MOF Containing Rod-Shaped Metal-Carboxylate/Hydroxyl SBU Exhibiting Afterglow Property at Low Temperature

WANG Peng-Fei*,[1,2] WANG Li-Jun[1]

([1]*School of Chemistry and Material Engineering, Chizhou University, Chizhou, Anhui* 247000, *China*)

([2]*State Key Laboratory of Coordination Chemistry, Nanjing University, Nanjing* 210023, *China*)

Abstract: A three-dimensional (3D) porous Zn(Ⅱ)-based framework, {[Zn_4(O-BTC)$_2$(H_2O)$_5$]·2DMF·0.5H_2O}$_n$ (**1**), which is constructed from a multifunctional tricarboxylate ligand, 2-hydroxyl-1,3,5-benzenetricarboxylic acid (HO-H_3BTC) and Zn(Ⅱ) salts was prepared. Complex **1** has been characterized by X-ray single-crystal diffraction, PXRD, elemental analysis, infrared spectroscopy, thermogravimetric analysis, and solid-state UV-Vis absorption spectra. Complex **1** exhibits a three-dimensional (3D) framework structure based on the rod-shaped Zn-carboxylate/hydroxyl secondary building unit (SBU). Solid-state luminescence studies showed that **1** exhibits intense blue emission at room temperature. Interestingly, **1** could exhibit afterglow property only under low temperature (10 K) condition. CCDC: 1856571.

Keywords: MOFs; rod-shaped metal-SBU; luminescent properties; afterglow

As a new class of multifunctional crystalline materials, metal-organic frameworks (MOFs) or porous coordination polymers (PCPs) have attracted considerable attentions, not only because of their intriguing

收稿日期:2018-07-22。收修改稿日期:2018-08-13。

国家自然科学基金(No.21101019)、安徽高校自然科学研究重点项目(No.KJ2018A0576)、安徽省大学生创新训练项目(No.201711306107)和南京大学配位化学国家重点实验室开放基金(No.SKLCC1805)资助。

*通信联系人。E-mail:njuwangpf@163.com

structures, but also for their potential applications in various fields such as gas storage and adsorption, catalysis, luminescence, magnetism, recognition of small molecules[1-8]. MOFs can be conventionally designed and constructed from many metal ions and/or metal-cluster units, and organic ligands containing functional groups through many methods. On the other hand, MOFs can also be considered as the combination of organic and inorganic hybrid materials. Moreover, luminescent MOFs have also been extensively studied due to their facile synthesis methods, tunable structures and applications in light-emitting diodes, flat panel displays, and similar devices, chemical sensors[9-11]. In particular, much interest has been extended to the luminescence performance of MOFs materials due to their inorganic-organic hybrid nature that offers unique advantages over other materials. Afterglow, also named long-lasting phosphorescence, which can last for an appreciable time after the removal of the excitation source, have attracted great attention since 2014[12-14]. However, the persistent luminescent materials have still relatively focused on rare-earth-containing inorganic materials, such as $SrAl_2O_4$:Eu^{2+} co-doped with Dy^{3+} ions[15-16]. An effective way of promoting phosphorescent properties on MOFs built of intrinsically fluorescent organic ligands is the inclusion of d^{10} closed shell metal ions, as the resulting MOFs materials contain excited states of ligand-centered and/or ligand-to-metal charge transfer nature, which may produce a long-lived emission[17-18]. Though many examples of fluorescent d^{10} electronic configuration complexes have been reported, phosphorescent materials remain more challenging and only a few studies have been published so far[19-20]. In this work we present the synthesis and characterization of a novel three-dimensional (3D) Zn-based MOF $\{[Zn_4(O\text{-}BTC)_2(H_2O)_5]\cdot 2DMF\cdot 0.5H_2O\}_n$ (**1**) based on a multifunctional ligand containing carboxylate and hydroxyl groups ($HO\text{-}H_3BTC$=2-hydroxyl-1,3,5-benzenetricarboxylic acid), which features the afterglow property at low temperature (10 K). In addition, the thermal stability, solid-state UV-Vis absorption spectra of **1** also have been studied.

1 Experimental

1.1 Materials and methods

The ligand ($HO\text{-}H_3BTC$) was synthesized according to the literature[21], and analytically pure $Zn(OAc)_2\cdot 2H_2O$, *N*,*N*-dimethylformamide (DMF) were purchased from Alfa Aesar Co. Ltd. and used without further purification. The IR spectrum was recorded on a Nicolet IS10 spectrometer with a KBr disk in the range of 4 000~400 cm^{-1}. Elemental analysis (C, H and N) was performed on a Thermo Fisher Flash 2000 elemental analyzer. Powder X-ray diffraction (PXRD) pattern was collected on a Rigaku Ultima-Ⅳ diffractometer with Cu $K\alpha$ (λ=0.154 06 nm). The measurement was performed over the 2θ range of 5°~50° at room temperature. The operating power was set at 30 mA, 40 kV. Thermogravimetric analysis (TGA) was carried out on a Shimadzu DTG-60 thermal analyzer under a N_2 atmosphere from room temperature to 800 ℃ at a heating rate of 10 ℃·min^{-1}. The solid-state UV-Vis absorption spectra were measured at room temperature using a Perkin-Elmer Lambda 900 UV-Vis spectrophotometer. Photoluminescence (PL) spectra, and time-resolved PL spectra experiments were conducted using an Edinburgh FLS980 fluorescence spectrometer. The PL quantum yield value at room temperature was estimated using a Teflon-lined integrating sphere in an Edinburgh FLS980 fluorescence spectrometer.

1.2 Synthesis of $\{[Zn_4(O\text{-}BTC)_2(H_2O)_5]\cdot 2DMF\cdot 0.5H_2O\}_n$ (1)

$Zn(OAc)_2\cdot 2H_2O$ (0.440 g, 2.0 mmol), $HO\text{-}H_3BTC$ (0.228 g, 1.0 mmol), *N*,*N*-dimethylformamide (DMF) (3.0 mL) and deionized water (27.0 mL) were added to a 50 mL Teflon reactor with stirring at room temperature (RT) for 60 min. Then it was sealed and kept under autogenous pressure at 140 ℃ for 48 h. The mixture was cooled slowly to RT, the precipitate was filtered off and mother liquors were left to slowly evaporate at RT. Well shaped block crystals were grown 3 months later. Then, they were collected by filtration and washed several times with water and dried in air at RT. Yield: 0.135 g, 15% based on $Zn(OAc)_2\cdot 2H_2O$. Elemental analysis Calcd. for

$C_{24}H_{29}N_2O_{21.5}Zn_4$(%): C, 30.31; H, 3.07; N, 2.95. Found (%): C, 30.65; H, 3.14; N, 3.01. IR (KBr pellets, cm^{-1}): 3 420 (s), 2 801 (m), 1 667 (s), 1 613 (vs), 1 553 (s), 1 470 (m), 1 420 (s), 1 370 (vs), 1 280 (s), 1 195 (w), 1 102 (m), 1 020 (w), 940 (w), 833 (m), 795 (m), 710 (m), 662 (w), 564 (w), 518 (w).

1.4 X-ray crystallography

The single-crystal diffraction data of **1** were collected on a Bruker APEX Ⅱ area detector with graphite monochromated Mo $K\alpha$ (λ=0.071 073 nm) at 296 K. After data collection, in the case an empirical absorption correction (SADABS) was applied[22]. The structure was then solved by the direct method using SHELXS-97[23] and refined on F^2 by full-matrix least-squares using SHELXL-97 program[24]. The coordinated water molecule (O1W) was disordered at two positions. The guest solvent molecules (DMF and H_2O) are also disordered over two positions. All non-hydrogen atoms were refined with anisotropic thermal parameters. The hydrogen atoms attached to the phenyl group carbon atoms were put in calculated positions, and the coordinated water hydrogen atoms were located from the Fourier maps. The crystallographic data for **1** are listed in Table 1. Selected bond lengths and angles are given in Table 2.

CCDC: 1856571.

Table 1 Crystal data and structure refinement for 1

Formula	$C_{48}H_{58}N_4O_{43}Zn_8$	Z	1
Formula weight	1 901.94	D_c / ($g\cdot cm^{-3}$)	1.511
Crystal system	Monoclinic	μ / mm^{-1}	2.342
Space group	$P2_1/c$	F(000)	958
a / nm	1.031 08(13)	GOF on F^2	1.06
b / nm	1.459 34(16)	R_1, wR_2^* [$I>2\sigma(I)$]	0.054 9, 0.131 7
c / nm	1.452 41(17)	R_1, wR_2^* (all data)	0.066 4, 0.133 2
β / (°)	107.038(3)	$(\Delta\rho)_{max}$, $(\Delta\rho)_{min}$ / ($e\cdot nm^{-3}$)	477, −529
V / nm^3	2.089 5(4)		

* $R_1=\sum||F_o|-|F_c||/\sum|F_o|$; $wR_2=[\sum w(F_o^2-F_c^2)^2/\sum w(F_o^2)^2]^{1/2}$

Table 2 Selected bond lengths (nm) and angles (°) for 1

Zn(1)-O(1)	0.208 9(3)	Zn(2)-O(1W)	0.201 2(9)	C(7)-O(3)	0.126 4(6)
Zn(1)-O(2)	0.198 9(3)	Zn(2)-O(3W)	0.213 5(8)	C(8)-O(4)	0.122 6(6)
Zn(1)-O(5)E	0.197 9(4)	Zn(2)-O(6)F	0.217 3(4)	C(8)-O(5)	0.124 7(6)
Zn(1)-O(7)A	0.200 4(3)	Zn(2)-O(2W)	0.210 0(4)	C(9)-O(6)	0.121 8(6)
Zn(1)-O(1)A	0.201 5(3)	C(1)-O(1)	0.131 4(6)	C(9)-O(7)	0.129 8(6)
Zn(2)-O(3)	0.210 5(4)	C(7)-O(2)	0.119 6(6)		
Zn(1)A-O(1)-Zn(1)	103.19(15)	O(7)A-Zn(1)-O(1)	142.71(14)	O(1W)-Zn(2)-O(6)F	113.4(3)
Zn(1)A-O(7)-Zn(2)C	139.08(16)	O(1)A-Zn(1)-O(1)	76.81(15)	O(2W)-Zn(2)-O(6)F	82.39(15)
Zn(2)-O(1W)-Zn(2)D	138.9(5)	O(1W)-Zn(2)-O(2W)	86.6(3)	O(3)-Zn(2)-O(6)F	97.82(14)
O(5)E-Zn(1)-O(2)	114.58(14)	O(1W)-Zn(2)-O(3)	148.6(3)	O(3W)-Zn(2)-O(6)F	99.18(15)
O(5)E-Zn(1)-O(7)A	114.34(15)	O(2W)-Zn(2)-O(3)	94.84(16)	O(1W)-Zn(2)-O(7)F	60.1(3)
O(2)-Zn(1)-O(7)A	89.52(13)	O(2W)-Zn(2)-O(1W)D	92.9(3)	O(2W)-Zn(2)-O(7)F	92.81(14)
O(5)E-Zn(1)-O(1)A	103.13(15)	O(3)-Zn(2)-O(1W)D	107.6(3)	O(3)-Zn(2)-O(7)F	150.64(14)
O(2)-Zn(1)-O(1)A	140.72(14)	O(1W)-Zn(2)-O(3W)	91.7(3)	O(1W)D-Zn(2)-O(7)F	100.2(3)
O(7)A-Zn(1)-O(1)A	84.51(14)	O(2W)-Zn(2)-O(3W)	178.04(16)	O(3W)-Zn(2)-O(7)F	87.15(14)
O(5)E-Zn(1)-O(1)	101.30(14)	O(3)-Zn(2)-O(3W)	86.13(16)	O(6)F-Zn(2)-O(7)F	55.23(12)
O(2)-Zn(1)-O(1)	85.20(13)	O(1W)D-Zn(2)-O(3W)	85.2(3)		

Symmetry codes: A: $-x+1$, $-y+2$, $-z$; B: x, $-y+3/2$, $z+1/2$; C: $x-1$, y, z; D: $-x+2$, $-y+2$, $-z$; E: x, $-y+3/2$, $z-1/2$; F: $x+1$, y, z.

2　Results and discussion

2.1　Description of crystal structure of 1

The single-crystal X-ray analysis of **1** reveals that it crystallizes in the monoclinic $P2_1/c$ space group, and there exist two crystallographically independent Zn(Ⅱ) ions, one O-BTC^{4-} anion, and two-half of coordinated water molecules (Fig.1). Interestingly, there are two types of five-coordinated Zn(Ⅱ) environment. The Zn1 atom is five-coordinated in a slightly distorted square-pyramidal coordination environment, which is coordinated by three carboxylate oxygen atoms (O2, O5E, O7A) from two O-BTC^{4-} ligands and two hydroxyl oxygen atoms (O1, O1A). The Zn2 atom adopts a slightly distorted trigonal bipyramidal coordination environment. The five binding sites around Zn2 are provided by two carboxylate oxygen atoms (O3, O6F) from two O-BTC^{4-} ligands and three coordinated water molecules (O1W, O2W, O3W). The Zn-O bond lengths fall in the 0.197 9(4)~0.217 3(4) nm range, and the O-Zn-O bond angles are 55.23(12)°~178.04(16)°. The O-BTC^{4-} ligand with the deprotonated hydroxyl group exhibits an uncommon coordination mode using its (κ^1-μ_2) hydroxyl oxygen atom to bridge two Zn(Ⅱ) ions, one (κ^1) carboxylate group to link one Zn(Ⅱ) ion, and two (κ^1-κ^1)-(κ^1-κ^1)-μ_4 carboxylate groups to bridge four Zn(Ⅱ) ions (Scheme 1). As a result, the O-BTC^{4-} ligand in **1** exhibits a unique (κ^1-μ_2)-(κ^1)-(κ^1-κ^1)-(κ^1-κ^1)-μ_5 pentadentate coordination mode which is completely different from it in previous work[25-26]. Zn1 and Zn1A ions are bridged by the hydroxyl oxygen atom (O1) to form a dimeric [Zn_2O_2] unit, which are further linked to Zn2 ions by the carboxylate groups to form an infinite Zn-carboxylate/hydroxyl secondary building unit (SBU) (Fig.S3). It can be described as an infinite rod-shaped SBU[27-28]. In the rod-shaped SBU, the Zn1…Zn1A through the hydroxyl oxygen atom, Zn1…Zn2 through the carboxylate group, and Zn1A … Zn2C through the carboxylate group distances are 0.321 6, 0.428 8 and 0.413 6 nm, respectively. Each rod-shaped SBU is linked to four adjacent rod-shaped SBUs through the O-BTC^{4-} ligands resulted in a three-dimensional framework with *pcu* type rod packing (Fig.2). As a result, the present 3D framework has 1D triangular channels that extend parallel to the

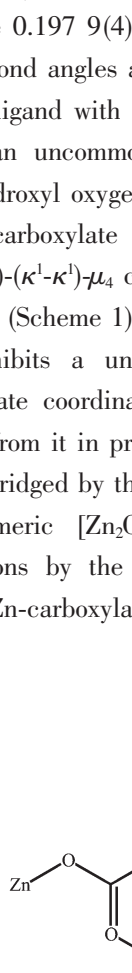

Scheme 1　Coordination mode of O-BTC^{4-} anion in **1**

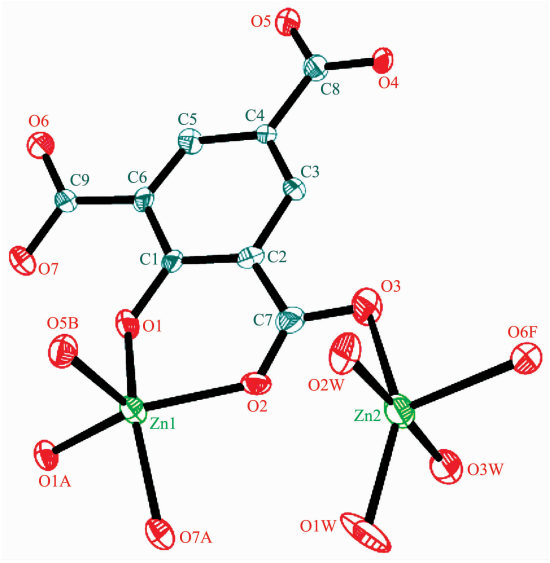

50% thermal ellipsoid probability; All H atoms and guest solvent molecules (DMF and H_2O) are omitted for clarity; Symmetry codes: A: $-x+1, -y+2, -z$; B: $x, -y+3/2, z+1/2$; C: $x-1, y, z$; D: $-x+2, -y+2, -z$; E: $x, -y+3/2, z-1/2$; F: $x+1, y, z$

Fig.1　Molecular structure of **1** in ORTEP view

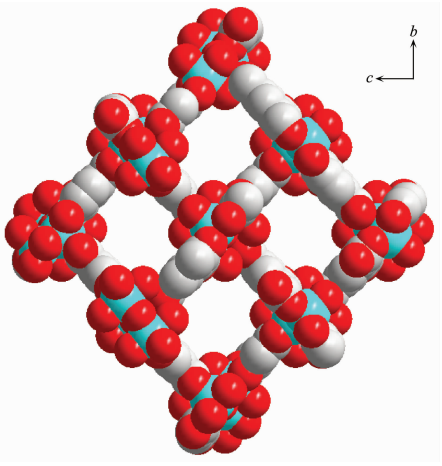

Fig.2　Space-filling view of the 3D framework structure of **1** along the *a*-axis

crystallographic *a*-axis, in which the coordination molecules protrude and solvent molecules reside in and interact with host framework through weak interactions. The accessible volume of the solvent molecules is 52.5% calculated by PLATON[29].

2.2 PXRD patterns, IR and thermal stability analysis of 1

The as-synthesized powder X-ray diffraction (PXRD) patterns obtained for the bulk sample of **1** are in good agreement with that of the simulated single-crystal data, indicating the phase purity of the bulk products. Meanwhile, the sharp diffraction peaks confirm the high crystallinity of **1**. The relatively high diffraction peaks of 2θ from 30° to 40° can be related to the preferred orientation of **1** (Fig.S1). The broad peak of the IR spectrum centered between 3 400 and 3 460 cm^{-1} is mainly attributed to the ν(OH) of the coordinated and lattice water molecules stretching vibrations (Fig.S2). The IR spectrum of **1** shows the characteristic bands of carboxylate groups of the O-BTC^{4-} ligand in 1 354~1 470 cm^{-1} for the symmetric stretching vibration and in 1 552~1 674 cm^{-1} for the asymmetric stretching vibration, all are in the general regions[30]. In addition, the vanished bands in 1 690~1 720 cm^{-1} for full deprotonation of the carboxylate groups of **1** implicate the full deprotonation of the HO-H_3BTC ligand on the reaction with metal ions. All these results match well the structure analysis of **1**. Thermogravimetric analysis (TGA) under N_2 atmosphere from 30 to 800 ℃ was employed to under-stand the thermal stability of **1**. As shown in Fig.3, sustained weight loss from room temperature to 600 ℃ may be attributed to the loss of lattice DMF and H_2O solvent as well as the coordinated water molecules, and the decomposition of the framework is completed. The ultimate residue may be zinc oxide (Obsd. 28.12%, Calcd. 32.10%).

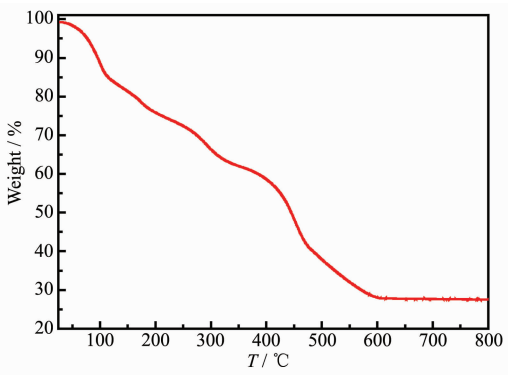

Fig.3 TG curve of **1** in nitrogen atmosphere

2.3 UV-Vis absorption spectra and luminescent properties of 1

The UV-Vis absorption spectroscopic properties for **1** and the organic ligand (HO-H_3BTC) are investigated since the HO-H_3BTC ligand is a chromophoric linker and present optical property. As given in Fig.4, the solid-state UV-Vis absorption spectra for the free HO-H_3BTC ligand and **1** are different at room temperature. The free ligand molecule (Fig.4) shows a relatively high intensity and spin-allowed broad band at *ca.* 262 nm. The main absorption can be ascribed to the $\pi\rightarrow\pi^*$ transition within the $S_0\rightarrow S_1$ state of HO-H_3BTC molecule. The main absorption band also appears for **1** but has been red-shifted to *ca.* 323 nm with broad band. The vanished shoulder peak and the red-shift phenomenon can be recognized as the results from the coordination interaction between the carboxylate groups of the HO-H_3BTC ligand and Zn(Ⅲ) ion[31]. The fluorescence excitation and emission spectra of **1** were examined in the solid state at 298 K. The emission spectra (Fig.5) of **1** displays single broad emission band centered at 437 nm under 365 nm excitation (Fig.S4). Compared to the emission of the free HO-H_3BTC ligand (λ_{max}=440 nm), the emission of **1** may be attributed to the intraligand ($\pi\rightarrow\pi^*$) fluorescent emission as the similar emission to that of the free HO-H_3BTC ligand[25], as reported for other Zn-MOFs constructed from organic ligands with conjugated

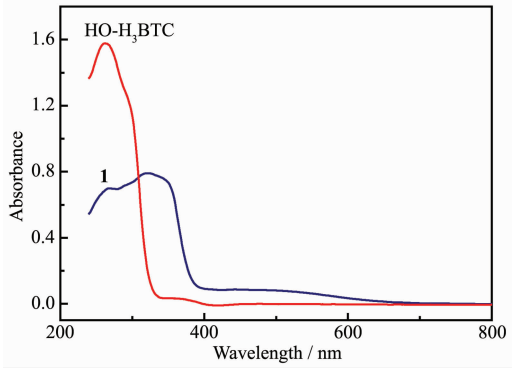

Fig.4 UV-Vis absorption spectra of **1** and HO-H_3BTC ligand in the solid state at room temperature

systems[32]. The absolute quantum yield was determined by means of an integrating sphere and the value obtained under an excitation of 365 nm is 8.5%. When the temperature is decreased from 298 K to 10 K, the maximum emission of **1** is red-shifted to 457 nm ($\Delta\lambda$= 20 nm). The coordination of Zn(Ⅱ) ions to the HO-H_3BTC ligand at low temperature (10 K) must allow more efficient intersystem crossing to the triplet state[33]. Interestingly, at low temperature (10 K) **1** shows an unexpected persistent emission after the removal of UV excitation. Time-resolved emission spectra (TRES) of **1** were recorded using different delays at 10 K (Fig. 6). The normalized spectra confirm that the emission of **1** undergoes a progressive slight red-shift while it gradually decreases, whereas the similar phenomenon could not be observed at 298 K.

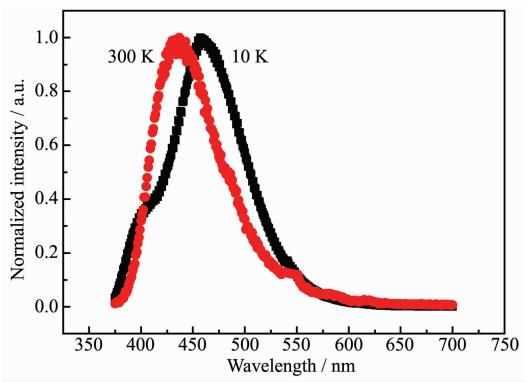

Fig.5　Solid-state luminescence spectra of **1** at 298 K and 10 K with λ_{ex}=365 nm

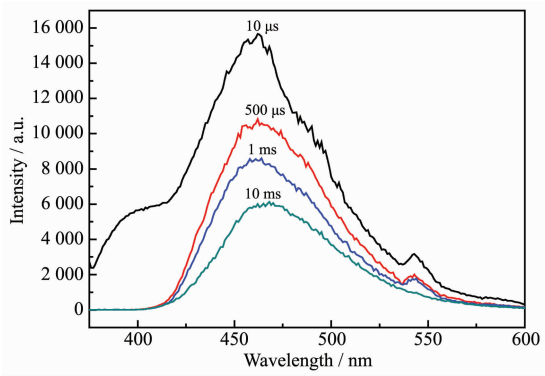

Fig.6　Time-resolved emission spectra at 10 K of **1** at different delays with λ_{ex}=365 nm

3　Conclusions

In summary, herein we report the design, synthesis and characterization of the luminescent properties of a Zn-based MOF consisting Zn(Ⅱ) metal and 2-hydroxyl-1,3,5-benzenetricarboxylic acid (HO-H_3BTC) ligand, $\{[Zn_4(O\text{-}BTC)_2(H_2O)_5]\cdot 2DMF\cdot 0.5H_2O\}_n$ (**1**). Complex **1** presents a 3D framework structure based on a rod-shaped Zn-carboxylate//hydroxyl secondary building unit (SBU). The result demonstrates that the multifunctional HO-H_3BTC ligand appears to be an appropriate candidate to generate diverse extended MOFs. In addition, **1** shows the afterglow property at low temperature.

Supporting information is available at http://www.wjhxxb.cn

References:

[1] Eddaoudi M, Kim J, Yaghi O M. et al. *Science*, **2002**,**295**:469-472

[2] Kitagawa S, Kitaura R, Noro S. *Angew. Chem. Int. Ed.*, **2004**, **43**:2334-2375

[3] Li B Y, Leng K Y, Ma S Q, et al. *J. Am. Chem. Soc.*, **2015**, **137**:4243-4248

[4] Chen B L, Xiang S C, Qian G D. *Acc. Chem. Res.*, **2010**,**43**:1115-1124

[5] Huang X D, Xu Y, Zheng L M, et al. *Angew. Chem. Int. Ed.*, **2018**,**58**:8577-8581

[6] Weng D F, Wang Z M, Gao S. *Chem. Soc. Rev.*, **2011**,**40**:3157-3181

[7] Liu F L, Li D, Tao J, et al. *Dalton Trans.*, **2018**,**47**:1407-1411

[8] Cui Y J, Chen B L, Qian G D, et al. *Acc. Chem. Res.*, **2016**, **49**:483-493

[9] Sun C Y, Wang X L, Li J, et al. *Nat. Commun.*, **2013**,**4**:2717-2723

[10]Chorazy S, Kumar K, Ohkoshi S, et al. *Inorg. Chem.*, **2017**,**56**:5239-5252

[11]Wang H, Lusting W P, Li J. *Chem. Soc. Rev.*, **2018**,**47**:4729-4756

[12]Cepeda J, Sebastian E S, Seco J M, et al. *Chem. Commun.*, **2016**,**52**:8671-8674

[13]Yuan S, Deng Y K, Sun D. *Chem. Eur. J.*, **2014**,**20**:10093-10098

[14]Yang X G, Yan D P. *Chem. Sci.*, **2016**,**7**:4519-4526

[15]LIU Ying-Liang(刘应亮), LEI Bing-Fu(雷炳富), KUANG Jin-Yong(邝金勇), et al. *Chinese J. Inorg. Chem.*(无机化学学报), **2009**,**25**(8):1323-1329

[16]Matsuzawa T, Aoko Y, Takeuchi N, et al. *J. Electrochem. Soc.*, **1996**,**143**:2670-2673

[17]Maragani R, Thomas M B, Misra R, et al. *J. Phys. Chem. A*, **2018**,**122**:4829-4837

[18]Howarth A J, Davies D L, Wolf M O, et al. *Inorg. Chem.*, **2014**,**53**:11882-11889

[19]Han L, Qin L, Xu L P, et al. *Inorg. Chem.*, **2013**,**52**:1667-1669

[20]Luo F, Sun G M, Zheng A M, et al. *Dalton Trans.*, **2012**,**41**:13280-13283

[21]Gao M J, Yang P, Wu J Z, et al. *CrystEngComm*, **2012**,**14**:1264-1270

[22]*SADABS* and *SAINT*, *Program for Data Extraction and Reduction*, Bruker AXS Inc., Madison, WI, USA, **2003**.

[23]Sheldrick G M. *SHELXS*-97, *Program for Crystal Structure Solution*, University of Göttingen, Germany, **1997**.

[24]Sheldrick G M. *SHELXL*-97, *Program for Crystal Structure Refinement*, University of Göttingen, Germany, **1997**.

[25]Yu M H, Hu T L, Bu X H. *Inorg. Chem. Front.*, **2017**,**4**:256-260

[26]WANG Peng-Fei(汪鹏飞). *Chinese J. Inorg. Chem.*(无机化学学报), **2018**,**34**(9):1747-1752

[27]Rosi N L, Kim J, Yaghi O M, et al. *J. Am. Chem. Soc.*, **2005**,**127**:1504-1518

[28]Wang Y L, Jiang Y L, Liu Q Y, et al. *Dalton Trans.*, **2012**,**41**:11428-11437

[29]Spek A L. *PLATON*: *A Multipurpose Crystallographic Tool*, Utrecht University, The Netherlands, **2001**.

[30]Nakamoto K. *Infrared and Raman Spectra of Inorganic and Coordination Compounds*. 6*th Ed*. New Jersey: John Wiley & Sons, Inc., **2009**:61-67

[31]Liu L, Dai J C. *Cryst. Growth Des.*, **2018**,**18**:4460-4469

[32]Cui Y J, Qian G D, Chen B L, et al. *Chem. Rev.*, **2012**,**112**:1126-1162

[33]Seco J M, Briones D, Cepeda J, et al. *Cryst. Growth Des.*, **2017**,**17**:3893-3906